

CONUS Contrail Frequency Estimated from RUC and Flight Track Data

D. P. Duda*

Hampton University, Hampton, VA USA

P. Minnis, P. K. Costulis

Atmospheric Sciences, NASA Langley Research Center, Hampton, VA USA

R. Palikonda

Analytical Services and Materials, Inc., Hampton, VA USA

Abstract

European Conference on Aviation, Atmosphere, and Climate

Friedrichshafen at Lake Constance, Germany

June 30 - July 3, 2003

* *Corresponding author:* David P. Duda, NASA Langley Research Center, Mail Stop 420, Hampton, VA 23681-2199 USA. Email: d.p.duda@larc.nasa.gov

CONUS Contrail Frequency Estimated from RUC and Flight Track Data

D. P. Duda^{*}
Hampton University, Hampton, VA USA

P. Minnis, P. K. Costulis
Atmospheric Sciences, NASA Langley Research Center, Hampton, VA USA

R. Palikonda
Analytical Services and Materials, Inc., Hampton, VA USA

Keywords: air traffic, contrail coverage

ABSTRACT: Estimates of contrail frequency and coverage over the continental United States (CONUS) are developed using hourly meteorological analyses from the Rapid Update Cycle (RUC) numerical weather prediction model and commercial air traffic data from FlyteTrax. The potential contrail frequency over the CONUS is computed directly from RUC analyses using a modified form of the classical Appleman criteria for persistent contrail formation. The potential contrail frequency is adjusted to account for the occurrence of thick cloudiness in possible regions of persistent contrail formation. The air traffic density data is then combined with the potential contrail frequency to estimate the expected contrail coverage. This estimate is compared with a direct satellite estimate of contrail coverage based on an empirical contrail detection algorithm.

1 INTRODUCTION

Contrails can affect the global atmospheric radiation budget by increasing planetary albedo and reducing infrared emission. Our current knowledge of the magnitude of these effects is extremely uncertain; two recent estimates of global linear contrail radiative forcing (Minnis et al., 1999; Ponater et al., 2002) differ by nearly two orders of magnitude. Global radiative forcing is difficult to estimate since it depends on several poorly known factors including the global mean contrail coverage. Current theoretical estimates of global contrail coverage (Sausen et al., 1998; Ponater et al., 2002) are tuned to early estimates of linear contrail coverage determined visually from infrared satellite imagery over the North Atlantic and central Europe (Bakan et al., 1994). The estimates differ based on the parameterization used to diagnose contrails and the numerical weather analyses employed to determine the ambient conditions. Recent estimates of contrail coverage over these areas from an objective detection algorithm (Mannstein et al., 1999; Meyer et al., 2002) are significantly smaller than those given by Bakan et al. (1994). Additionally, a comparison of the empirical contrail coverage of Sausen et al. (1998) with contrail coverage analyses of Advanced Very High Resolution Radiometer (AVHRR) data taken over the continental United States (CONUS) (Palikonda et al., 1999) show they compare well in overall magnitude of coverage, but differ in spatial distribution. These results illustrate the current uncertainty in contrail coverage estimation, a key component in the determination of contrail climate effects.

Development of reliable methods for diagnosing persistent contrails and their physical and radiative properties from numerical weather analyses is essential for predicting future contrail climate impacts. Because air traffic is expected to grow by 2 to 5% annually (Minnis et al., 1999), it is becoming more important to estimate contrail coverage accurately.

To address this concern, we use actual flight data and coincident meteorological data to compute an estimate of contrail coverage over the CONUS. This estimate is compared with a satellite retrieval of contrail coverage based on an objective contrail detection algorithm.

^{*} *Corresponding author:* David P. Duda, NASA Langley Research Center, Mail Stop 420, Hampton, VA 23681-2199 USA. Email: d.p.duda@larc.nasa.gov

2 DATA

2.1 Air traffic data

Commercial air traffic data from the FlyteTrax product (FT; FlyteComm, Inc., San Jose, CA) as compiled by Garber et al. (2003) were used to determine air traffic density over the continental United States during September 2001 and November 2001. The database consists of 2 or 5-minute readings of aircraft (flight number, aircraft type), position (latitude, longitude, altitude), and heading for every non-military flight over the USA and a portion of Canada, including related transoceanic flights. Although the FT database does not include military flights, it contains most of the air traffic over the CONUS. Air traffic densities were tabulated on a $1^\circ \times 1^\circ$ grid that extends from 20°N to 50°N in latitude, and from 135°W to 60°W in longitude.

2.2 Meteorological data

Atmospheric profiles of temperature and humidity were derived from the 40-km resolution, 1-hourly Rapid Update Cycle (RUC) analyses (Benjamin et al., 1998) in 25-hPa intervals from 400 hPa to 150 hPa. The RUC data were linearly interpolated at each pressure level to a $1^\circ \times 1^\circ$ grid that extends from 25°N to 56°N in latitude, and from 129°W to 67°W in longitude.

The RUC analyses at 00 UTC and 12 UTC were not used in this study to insure that the humidity fields for each hour were consistent. Before February 2002, a “quick-look” version of the 00 UTC and 12 UTC analyses was used. This version of the analysis does not include all available radiosonde data, and is noticeably drier in the upper troposphere than the analyses from other hours.

A major revision to the operational RUC model was implemented on 17 April 2002. The RUC20 model with 20-km horizontal resolution replaced the RUC40 model with 40-km horizontal resolution. The primary motivation for changes in the RUC model was improved quantitative precipitation forecasts. As a result, several changes in the way the model handles upper tropospheric moisture were added, including a more sharply defined tropopause, and the removal of most ice supersaturations for pressure levels less than 300 hPa (Benjamin et al., 2002).

The effect of these changes was to make the upper troposphere drier than in the RUC40. Thus, the relative humidity thresholds used to make the contrail diagnoses had to be changed for the RUC20. A serendipitous discovery of nearly simultaneous RUC20 (19 UTC) and RUC40 (20 UTC) model analyses from 26 May 2002 was used to relate the RUC20 humidity data to the older RUC40 data. The relative humidities with respect to ice (RHI) from the RUC20 analyses were adjusted based a level-by-level comparison of the mean RHI computed from the RUC20 and RUC40 data.

2.3 Satellite data

The satellite datasets for deriving contrail and cloud coverage consist of infrared radiances from the Sun-synchronous *NOAA-16* AVHRR 1-km imager (10.8 and 12.0 μm) and multispectral 1-km data from the MODERate Resolution Imaging Spectroradiometer (MODIS) on the *Terra* satellite. Half-hourly infrared data from the Geostationary Operational Environmental Satellite (*GOES* 8) imager (4-km resolution, 10.8 and 12.0 μm) was also used for tracking contrails over the continental US.

3 METHOD

Persistent contrail formation was computed according to the classical criteria of Appleman (1953) using the RUC profiles of temperature and humidity. The contrail formation algorithm follows Schrader (1997), modified with the aircraft propulsion efficiency parameter (η) of Busen and Schumann (1995). The mean value of the propulsion efficiency assumed for the present commercial fleet was 0.30 (Sausen et al., 1998). The saturation vapor pressure coefficients of Alduchov and Eskridge [1996, AERW(50,-80) and AERWi(0,-80)] were used to compute saturation vapor pressure over water and ice.

According to classical contrail formation theory, contrails can persist when the ambient air is supersaturated with respect to ice (that is, the environmental RHI is greater than 100 percent), but not with respect to water. In Sausen et al. (1998), the use of ECMWF reanalysis data required a contrail parameterization to compute persistent contrail coverage since the RHI in the ECMWF model rarely exceed 100 percent. The RUC model contains a sophisticated cloud and moisture scheme that allows for ice-supersaturation. Assuming that the RUC upper tropospheric moisture variables are accurate, we can follow a much simpler statistical evaluation of potential persistent contrail frequency. For each $1^\circ \times 1^\circ$ grid location where the criterion for persistent contrails occurs at any level from 400 hPa to 150 hPa, a persistence indicator is given a value of 1 for each hourly analysis. The indicator equals zero when none of the levels satisfies the persistence criterion. The potential contrail frequency (PCF) over a time period becomes simply the frequency of occurrence of the persistence indicator at a particular location.

To compute the actual contrail coverage, the PCF must be multiplied by the air traffic density. For an initial estimate, we will assume that the air traffic density is sparse enough to relate contrail fractional coverage to traffic density linearly. An unknown quantity is the mean fractional persistent contrail coverage within an area resulting from a single flight track (c_{ft}). In this study c_{ft} was tuned so that the US mean contrail coverage would match monthly satellite-based contrail coverage estimates (Palikonda et al., 2003). The value of c_{ft} varied by only 5 percent between September 2001 (5.86×10^{-5}) and November 2001 (5.57×10^{-5}). Since the mean area of a $1^\circ \times 1^\circ$ grid cell in the midlatitudes is approximately $10,000 \text{ km}^2$, the mean coverage from a single flight track within a grid cell would be about 0.6 km^2 . No overlap of the contrails is assumed because the coverage is tuned to a satellite estimate and contrail altitude is not considered in this study. The total persistent contrail coverage (c_{sum}) in a grid cell is simply

$$c_{sum} = P \times c_{ft} \times n \quad (1)$$

where P is the potential contrail frequency, c_{ft} is the mean fractional persistent contrail coverage within a grid cell from a single flight track, and n is the total number of flight tracks within a grid cell. To account for the effects of natural cloudiness obscuring the detection of contrails, the persistence indicator used in the computation of PCF was set to zero whenever a grid box was more than 50 percent covered by high cloud.

4 RESULTS AND DISCUSSION

4.1 Potential contrail frequency

Figures 1 and 2 present the potential contrail frequency computed for September 2001 and November 2001 respectively. RUC analyses were available for only 26 of 30 possible days during each month. In both figures, the region with the highest PCF was the Pacific Northwest, where values reach 0.33 in September and 0.50 in November. Another region of high frequency in November is the eastern Midwest portion of the US. The overall distribution and the magnitude of potential contrail frequency changed dramatically as a result of changes in the synoptic-scale weather patterns between September and November. The mean PCF for grid points over the continental US was 0.118 in September and increased to 0.272 in November.

September 2001 Pot. Pers. CT Freq. (in percent) eta = 0.3

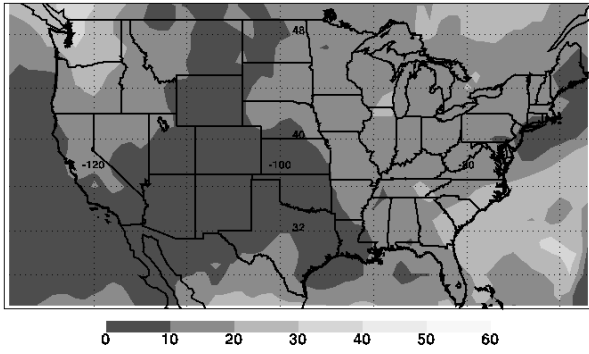


Figure 1. Potential persistent contrail frequency computed from RUC analyses for September 2001.

November 2001 Pot. Pers. CT Freq. (in percent) eta = 0.3

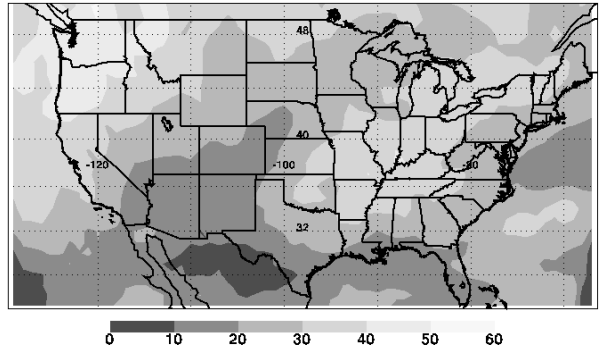


Figure 2. Potential persistent contrail frequency computed from RUC analyses for November 2001.

November 2001 Pot. Pers. CT Freq. in N-16 overpass areas (in percent) eta = 0.3

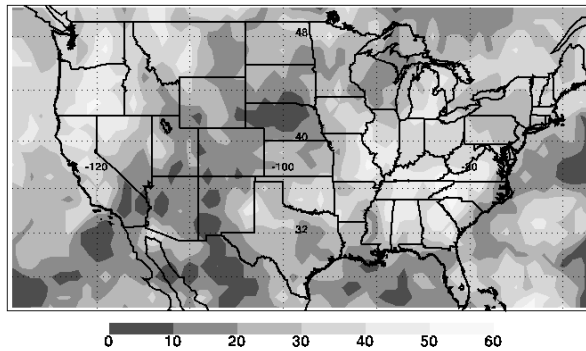


Figure 3. Potential persistent contrail frequency computed from RUC analyses during available RUC afternoon overpass times for November 2001.

Figure 3 presents the PCF computed for November 2001 during 54 afternoon overpasses of the *NOAA-16* satellite. To approximate the satellite coverage in the calculation of the contrail frequencies, only grid points within ± 12 degrees of longitude of the sub-satellite point at 37°N were counted during each overpass. Although the mean potential contrail frequency computed for the CONUS region was almost identical to the monthly average (0.269), the distribution of PCF shows much more variability due to the limited sample size.

To check the quality of the RUC-based potential contrail frequencies, they were compared to a daily, manual analysis of CONUS contrail coverage based on 4-km *GOES-8* imagery. The $10.8 \mu\text{m}$ minus $12.0 \mu\text{m}$ brightness temperature difference images between 1045 UTC and 0045 UTC were examined for the occurrence of contrails within each state of the US. For each day of the analysis, a persistence indicator value of 1 was given for each state in which at least one contrail appeared. The contrail frequency for each state is simply the percentage of the total analysed days with contrail occurrence. The mean of the contrail frequency for all states in the CONUS region was defined as the observation index. The comparison is shown in Figure 4.

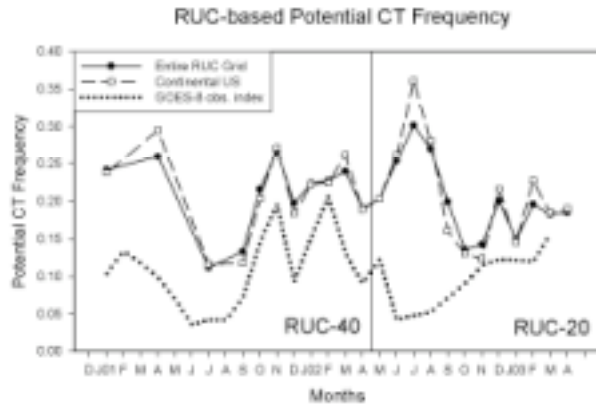


Figure 4. Time series of potential contrail frequency computed from RUC analyses between December 2000 and April 2003. The solid line is the frequency computed for all RUC grid points, while the dashed line only includes grid points over the CONUS. The dotted line indicates the *GOES-8* observation index.

As expected, the contrail frequencies computed from the RUC model are higher than the observation index since the index is based on observations of 4-km resolution data that miss narrow contrails. In addition, any satellite-based estimate is affected by obscuration by natural clouds. Both the potential contrail frequencies and the observation index show a similar seasonal cycle except for the summer months of 2002 when the RUC20 model data was used. The overestimate in potential contrail frequency during this period is likely the result of differences in the convective parameterization between the RUC40 and the RUC20.

November 2001 SIMULATED Pers. CT Coverage from N-16 (in percent) $\eta = 0.3$
(LINEAR relation between coverage and air traffic)

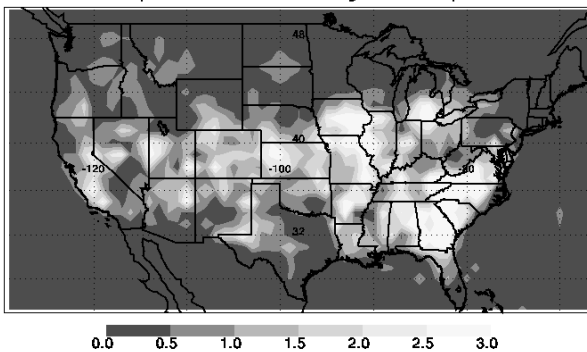


Figure 5. Persistent contrail coverage computed for November 2001 assuming linear relationship between contrail coverage and air traffic density.

November 2001 SIMULATED Pers. CT Coverage from N-16 (in percent) $\eta = 0.3$
(SQUARE ROOT relation between coverage and air traffic)

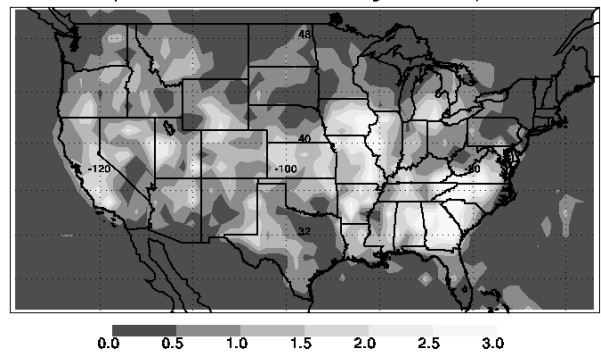
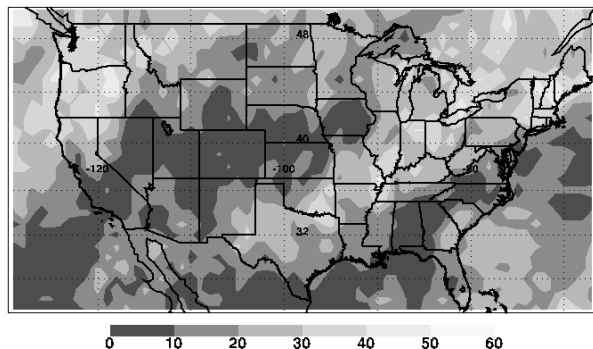


Figure 6. Persistent contrail coverage computed for November 2001 assuming square root relationship between contrail coverage and air traffic density.

4.2 Contrail coverage

Figure 5 shows a plot of persistent contrail coverage c_{sum} (assuming contrail coverage is proportional to air traffic density) computed for November 2001. The contrail coverage is heavily influenced by the air traffic density pattern, and is similar in appearance to Sausen et al. (1998), with a maximum of more than 0.03 in the eastern half of the CONUS, and relatively little coverage in the northern Great Plains. The mean theoretical contrail coverage for the CONUS is 0.0092. In high air traffic regions, however, contrail coverage may not be linearly related to air traffic density due to “saturation” effects (i.e. competition for moisture or overlapping of contrails in air traffic corridors may limit the number of linear contrails that are visible by satellite). If a square-root relation between coverage and air traffic is assumed, the contrail coverage is less dependent on air traffic density (Figure 6). High cloud coverage (cloud tops > 5 km) for November 2001 (see Figure 7) was derived from *Terra* MODIS multispectral observations (Minnis et al., 2002), and was used in the estimate of c_{sum} to account for the effects of natural cloudiness obscuring the detection of contrails.

November 2001 High Cloud Coverage from Terra (in percent)



NOAA-16 derived CT coverage for November 2001 (in percent)

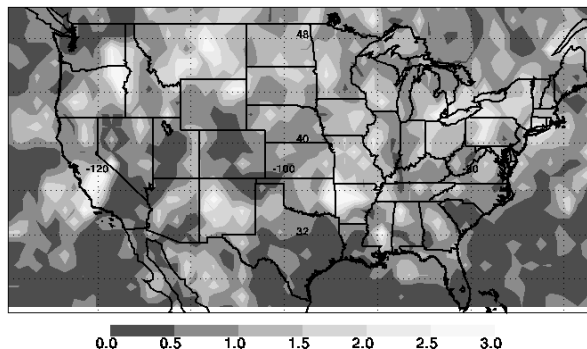


Figure 7. Cloud coverage above 5 km computed NOAA-from Terra morning overpass measurements.

Figure 8. Contrail coverage computed from 16 afternoon overpasses for November 2001 using an objective analysis.

The satellite-based CONUS contrail coverage estimates for September and November 2001 (Palikonda et al., 2003) used NOAA AVHRR data and an objective contrail detection algorithm (Mannstein et al., 1999) to compute contrail coverage. The results from both September (not shown) and November (Figure 8) suggest that the contrail coverage may be more dependent on the potential contrail coverage (in other words, the environmental conditions) than the estimates in Figures 5 and 6 suggest. Several unresolved factors may account for this difference. These factors include the likelihood that contrail coverage is non-linearly related to air traffic density, and the contrail coverage saturates in high traffic areas. Also, the current analysis neglects the advection of contrails and assumes that the RUC40 analyses provide an accurate characterization of the upper tropospheric temperature and moisture fields over the entire domain.

5 CONCLUSIONS AND FUTURE WORK

The simulated persistent contrail coverage presented here is heavily influenced by the air traffic pattern, similar to earlier studies. The contrail coverage computed from NOAA-16 imagery, however, is more closely related to the potential contrail frequency (and high cloud coverage) than air traffic density. Thus, the coverage of *line-shaped* contrails is non-linearly related to air traffic, and “saturation” effects are important in high traffic areas. Additional tuning and testing of the contrail coverage estimates is in progress. More work is necessary to compare satellite-based estimates of contrail coverage with potential coverage diagnosed from RUC analyses. The effects of flight altitude, synoptic-scale vertical motions, contrail advection, and RUC uncertainties have not been included in this study. More NOAA-16 data must be analysed since a sample size of one or two months is still too small. The results from other satellite platforms such as NOAA-17 (with a crossover time approximately 4 hours before NOAA-16) would help determine whether the relation between contrail coverage and air traffic changes throughout the day.

REFERENCES

- Alduchov, O. A., and R. E. Eskridge, 1996: Improved Magnus form approximation of saturation vapor pressure. *J. Appl. Meteor.* 35, 601–609.
- Appleman, H., 1953: The formation of exhaust condensation trails by jet aircraft. *Bull. Amer. Meteor. Soc.* 34, 14–20.
- Bakan, S., M. Betancor, V. Gayler, and H. Grassl, 1994: Contrail frequency over Europe from NOAA-satellite images. *Ann. Geophys.* 12, 962–968.
- Benjamin, S. G., J. M. Brown, K. J. Brundage, B. E. Schwartz, T. G. Smirnova, and T. L. Smith, 1998: The operational RUC-2. In: *Preprints, 16th AMS Conference on Weather Analysis and Forecasting*, Phoenix, AZ. American Meteorological Society, Boston, USA, pp. 249-252.

- Benjamin, S. G., J. M. Brown, K. J. Brundage, D. Dévényi, G. A. Grell, D. Kim, B. E. Schwartz, T. G. Smirnova, T. L. Smith, S. S. Weygandt, and G. S. Manikin, 2002: RUC20 – The 20-km version of the Rapid Update Cycle. *NWS Technical Procedures Bulletin No. 490*.
- Busen, R., and U. Schumann, 1995: Visible contrail formation from fuels with different sulfur contents. *Geophys. Res. Lett.* *22*, 1357–1360.
- Garber, D. P., P. Minnis, and K. P. Costulis, 2003: A USA commercial flight track database for upper tropospheric aircraft emission studies. In: *Proceedings of the European Conference on Aviation, Atmosphere, and Climate*, June 30 - July 3, 2003, Friederichshafen at Lake Constance, Germany.
- Mannstein, H., R. Meyer, and P. Wendling, 1999: Operational detection of contrails from NOAA-AVHRR-data. *Int. J. Remote Sensing* *20*, 1641–1660.
- Meyer, R., H. Mannstein, R. Meerkötter, U. Schumann, and P. Wendling, 2002: Regional radiative forcing by line-shaped contrails derived from satellite data. *J. Geophys. Res.* *107* (D10), doi: 10.1029/2001JD000426, 31 May 2002.
- Minnis, P., U. Schumann, D. R. Doelling, K. M. Gierens, and D. W. Fahey, 1999: Global distribution of contrail radiative forcing. *Geophys. Res. Lett.* *26*, 1853–1856.
- Minnis, P., D. F. Young, B. A. Wielicki, D. P. Kratz, P. W. Heck, S. Sun-Mack, Q. Z. Trepte, Y. Chen, S. L. Gibson, R. R. Brown, 2002: Seasonal and diurnal variations of cloud properties derived for CERES from VIRS and MODIS data. In: *Proceedings of the 11th AMS Conference on Atmospheric Radiation*, June 3 - 7, 2002, Ogden, Utah, USA, pp.20-23.
- Palikonda, R., P. Minnis, D. R. Doelling, P. W. Heck, D. P. Duda, H. Mannstein and U. Schumann, 1999: Potential radiative impact of contrail coverage over continental USA estimated from AVHRR data. In: *Preprints, 10th AMS Conference on Atmospheric Radiation*, June 28-July 2, 1999, Madison, Wisconsin. American Meteorological Society, Boston, USA, pp. 181-184.
- Palikonda, R., D. N. Phan, and P. Minnis, 2003: Contrail coverage over the USA derived from MODIS and AVHRR data. In: *Proceedings of the European Conference on Aviation, Atmosphere, and Climate*, June 30 - July 3, 2003, Friederichshafen at Lake Constance, Germany.
- Ponater, M., S. Marquart, and R. Sausen, 2002: Contrails in a comprehensive global climate model: Parameterization and radiative forcing results. *J. Geophys. Res.* *107*, 10.1029/2001JD000429, 3 July 2002.
- Sausen, R., K. Gierens, M. Ponater, and U. Schumann, 1998: A diagnostic study of the global distribution of contrails. Part I: Present day climate. *Theor. Appl. Climatol.* *61*, 127–141.
- Schrader, M. L., 1997: Calculations of aircraft contrail formation critical temperatures. *J. Appl. Meteor.* *36*, 1725–1729.